Title

Combining femtosecond laser annealing and shallow ion implantation for local color center creation in diamond

Journal

Applied Physics Letters, 122(23)

ISSN

0003-6951

Authors

Engel, Johannes

Jhuria, Kaushalya

Polley, Debanjan

et al.

Publication Date

2023-06-05

DOI

10.1063/5.0143922

RESEARCH ARTICLE | JUNE 06 2023

Combining femtosecond laser annealing and shallow ion implantation for local color center creation in diamond

Johannes Engel ; Kaushalya Jhuria ; Debanjan Polley ; Tobias Lühmann; Manuel Kuhrke ; Wei Liu ; Jeffrey Bokor ; Thomas Schenkel ; Ralf Wunderlich

Appl. Phys. Lett. 122, 234002 (2023)
https://doi.org/10.1063/5.0143922

Applied Physics Letters ARTICLE pubs.aip.org/aip/apl

Combining femtosecond laser annealing and shallow ion implantation for local color center creation in diamond

Cite as: Appl. Phys. Lett. **122**, 234002 (2023); doi: 10.1063/5.0143922
Submitted: 27 January 2023 · Accepted: 26 May 2023 ·
Published Online: 6 June 2023

Johannes Engel,[1] Kaushalya Jhuria,[2] Debanjan Polley,[3,4] Tobias Lühmann,[1] Manuel Kuhrke,[1] Wei Liu,[2] Jeffrey Bokor,[3,4] Thomas Schenkel,[2] and Ralf Wunderlich[1,2,a)]

AFFILIATIONS

[1]Faculty of Physics and Earth Sciences, Felix Bloch Institute for Solid State Physics, Applied Quantum Systems, Leipzig University, Linnéstrasse 5, Leipzig 04103, Germany
[2]Accelerator Technology and Applied Physics Division, Lawrence Berkeley National Laboratory, Berkeley, California 94720, USA
[3]Materials Sciences Division, Lawrence Berkeley National Laboratory, Berkeley, California 94720, USA
[4]Department of Electrical Engineering and Computer Sciences, University of California, Berkeley, California 94720, USA

[a)]Author to whom correspondence should be addressed: ralf.wunderlich@uni-leipzig.de

ABSTRACT

A common technique for color center creation in wideband gap semiconductors employs ion implantation and a subsequent thermal annealing. In general, this annealing process is conducted in an vacuum oven. Here, we exploit the annealing based on femtosecond laser pulses. For that purpose, we implant fluorine ions at 54 keV and chlorine ions at 74 keV in diamond and perform micrometer precise annealing using focused femtosecond laser pulses at 800 ± (30) nm with different pulse numbers and repetition rates. In this way, we were able to create shallow spots with color centers of varying brightness.

Color centers in wideband gap semiconductors promise a broad spectrum of applications as single-photon emitters or solid state spin qubits, like the nitrogen vacancy (NV) center in diamond or the divacancy (DV) in silicon carbide (SiC).[1–3] Such color centers can be created by ion implantation in the desired host material.[4,5] Often a subsequent thermal annealing process is needed to form the final defect structure since a vacancy is involved or the implanted ion has to be incorporated in the crystal structure.[6–8] While the implantation can be performed spatially in a very localized manner, the standard annealing procedure heats the entire sample.[9–12] This is very time-consuming and makes it difficult to systematically investigate the influence of the annealing temperature on the color center formation. Already decades ago, ultra-short laser pulses were investigated for the creation of color centers in crystals like LiF or glasses.[13,14] In recent years, the idea arises to utilize ultrashort pulsed lasers for the color center creation in materials like diamond, SiC, or gallium nitride (GaN) in the context of quantum applications.[15,16] In the beginning, these pulses were used for a local vacancy creation with a resolution of a few hundred of nanometers, albeit a bulk postannealing process was still required.[17] Later, the same technique was adapted for local heating inside the sample to achieve a localized vacancy diffusion and, therefore, a creation of vacancy-related color centers.[18] In particular, NV centers were created about 50 μm below the surface of a diamond sample, which contains homogeneously distributed substitutional nitrogen (1.8 ppm). Also the creation of high-density NV center layers about 15 μm below the surface was reported.[19] The same technique was applied to color centers in 4H- and 6H-SiC.[20–23] Typically, the reported generation of color centers in such materials takes place in the bulk, and so far only a few publications are known for fabrication near or at the surface.[15] In addition, the fabricated color centers are formed by "intrinsic" defects, meaning vacancies or atom species which are already present during the crystal growth. Therefore, such defects are randomly distributed inside the sample. For many applications, it would be favorable to extend this approach to "extrinsic" defects and also to produce the color centers near the surface.[24–29] We propose that this can be achieved by low energy shallow ion implantation, followed by laser annealing. Here, we use diamond as an exemplary wide bandgap host material to study such an approach, as it has

a rich zoo of potential color centers.[30–32] More precisely, we implant the two lightest halogens, namely, fluorine and chlorine. The first one is known to efficiently form a color center, while for the latter one, no color center is reported in the literature.[33] Since both atoms are chemically similar, chlorine is used as a control implantation, where only damage is created in the crystal lattice. It enables us to compare the laser pulse driven formation of fluorine related color centers with the effects of such a treatment on a pre-damaged area without color center formation. The F-related color center is attributed to a vacancy-related configuration according to preliminary *ab initio* simulations.[34] For this purpose, it is denoted as FV, even though the internal structure of this defect is not yet clearly understood, and this is not in the focus of this study. The center exhibits a bright photoluminescence (PL) and simple PL spectrum consisting essentially of only one broad band, thus allowing relatively easy fitting of the PL data.[4] Unlike the NV center, for example, it is also not an intrinsically occurring defect in artificially produced diamonds. Thus, it can be easily correlated with the ion implantation.

The experiment was conducted on a commercially available type-IIa single-crystal diamond produced by chemical vapor deposition (CVD) and nominal concentrations of both substitutional nitrogen and boron impurities below the 5 ppb level ($2 \times 2 \times 0.5\,\mathrm{mm}^3$) ("electronic grade" from *ElementSix*).

The preparation of the sample can be divided in the following steps (Fig. 1). First, two separate square-shaped areas are implanted with 54 keV fluorine and 74 keV chlorine, respectively. The fluences were 1×10^{13} cm^{-2} for both implantations. The corresponding implantation profiles simulated by the SRIM program can be found in Figs. 2(a) and 4(a) and show an average penetration depth of about 60nm (41nm).[35] The sample was cleaned for 4 h in a 1 : 3 : 1 mix of concentrated nitric acid, sulfuric acid, and perchloric acid (70%), and no post-annealing was applied to the sample. In a final preparation step, the implanted areas were locally illuminated using a commercial amplifier laser system (RegA 9000, from Coherent) with variable repetition rate, a center wavelength of 800 nm (∼±30nm linewidth), and a fixed pulse width of ∼80 fs. We achieve a spot size of about 2 μm at the sample surface using a 50× objective (from Mitutoyo, NA 0.65). Three different repetition rates (252, 100, and 10 kHz), six different pulse energies (79, 60, 48, 36, 28, and 16 nJ) (measured in front of the 50× objective which has about 15% transmission), and six different numbers of pulses (1×10^7, 1×10^6, 1×10^5, 5×10^4, 1×10^4, and 5×10^3) were used. The pulse energies were chosen to be well below the graphitization threshold, which was previously found to be about 150 nJ on the very same sample. This was evaluated by irradiating a series of energy-dependent laser pulses in a higher energy range onto a pristine part of the sample surface. The number of pulses was determined by a shutter with an open/close time of 10ms. Due to the partial blocking of the laser beam during opening and closing, lower pulse energies as specified can result for about 2500 , 1000, and 100 pulses according to different repetition rates.

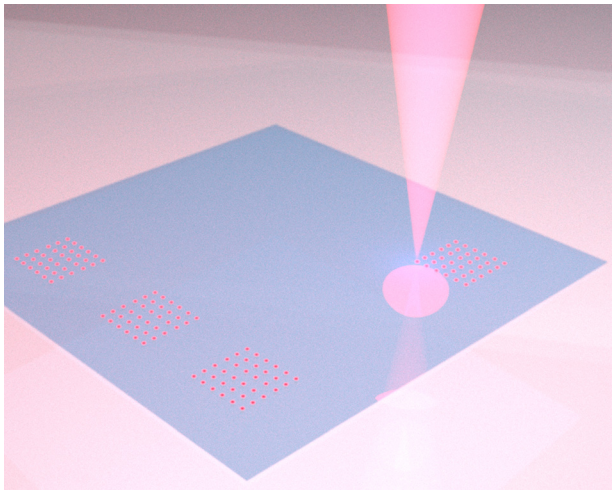

FIG. 1. Artistic illustration: Top view on the sample surface. The last step of the sample preparation is shown, where a focused and pulsed fs laser creates arrays of color center spots (red) in a previously ion implanted area (blue). For the implantation, we use either a fluorine or chlorine ion beam shaped by a square aperture. This provides constituents for the potential formation of color centers at a depth of less than 100nm below the diamond surface.

The annealing spots were grouped in three rectangular patterns for the different repetition rates. Such a pattern consists of 6×6 spots, where the pulse energy is varied in the x axis (lines) and the pulse numbers in the y axis (columns). The analysis was done with a home-built confocal microscope (100× objective, NA 0.95) in combination with a HORIBA Jobin Yvon spectrometer (150 mm^{-1} grating). Figure 2(c) shows a false color image of a confocal scan of one annealing pattern. The photoluminescence (PL) was collected under an excitation wavelength of 532 nm at a power of circa 135 μW. A 532 nm notch filter was used for the collection of the PL spectra and an additional 550 nm LP for the record of confocal scan images. The spectrum of each individual annealing spot was acquired for 3 min after an x, y, z optimization for the maximal PL intensity. Additionally, a corresponding background spectrum was acquired for each spot. Figures 2(d)–2(i) show examples of the accumulated spectra for six different pulse energies at 252 kHz and 1×10^7 pulses for fluorine implantation.

The experimental results of the femtosecond (fs) laser treatment on the fluorine and chlorine implanted areas are discussed below, starting with the former. Please note that all normalizations used are consistent and the PL intensities in the graphs can be compared with each other.

As it can be seen for the pattern created at 252 kHz in Fig. 2(c), not all parameter combinations of the pulse energy and pulse number lead to the formation of a bright PL spot. In particular, there is no PL spot visible for the lower pulse energies and lower pulse numbers [upper right region in Fig. 2(c)]. For the combinations leading to a PL spot, an increasing PL intensity with increasing energy/pulse number can be observed. For example, at a repetition rate of 252 kHz with 10^7 pulses, a clear monotonic trend of the PL intensities with varying pulse energy can already be seen in the spectra given in Figs. 2(d)–2(i). This is intuitive, since with increasing pulse energy at a constant repetition rate, there is also a higher energy input and, thus, also more heating power available. A closer look at the spectral shape of the PL reveals that the spectrum can be divided into two dominant parts [Fig. 3(a)]. For this, we compare the spectrum with the ensemble spectrum of F related color centers created by ion implantation (45 keV, 1.5×10^{12} cm^{-2}) and subsequent annealing (1200 °C, 2h) on a similar sample. The PL spectrum thus obtained was used as the FV reference spectrum for the laser-generated PL spots and fitted to their PL spectra

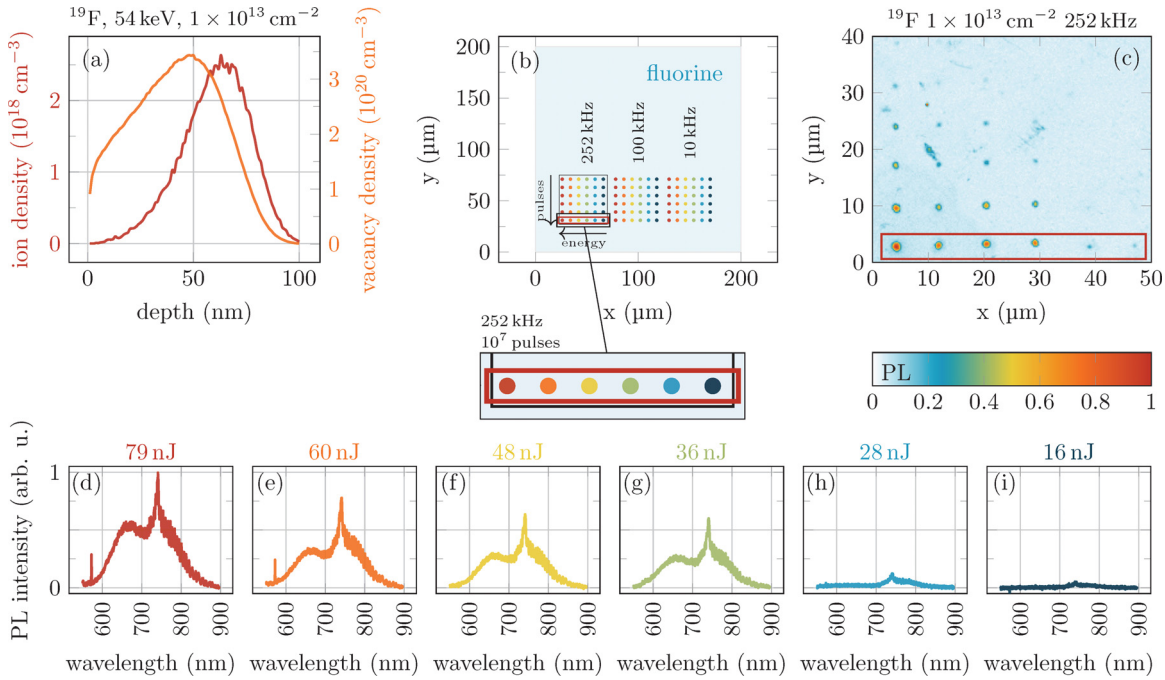

FIG. 2. Information and data for the fluorine implantation and laser treatment: (a) the depth dependent ion density for fluorine (54keV, 1 × 10^{13}cm^{-2}). (b) A sketch of the implantation region and the positions of different laser treated spots. The spots are arranged in three squares corresponding to different lases pulse repetition rates. The spots are color coded corresponding to their pulse energy. The pitch for the spots is 8μm. (c) A confocal scan image [compare black square and red rectangle in (b) for one set of parameters (pulse energy, pulse number, and repetition rate)]. The red rectangle marks the spots with different pulse energies and fixed pulse numbers (10^7). The corresponding spectral resolved PL for each spot was acquired (d)–(i).

[Fig. 3(a), blue curve]. The small discrepancy of both spectral shapes is attributed to the damage caused by the ion implantation during the pretreatment. Subsequently, the fit is subtracted from the spectrum. The remaining PL spectrum shows the clear signature of neutral vacancies [V^0, zero phonon line (ZPL) at 741 nm], namely, GR1 centers (yellow).[36,37] This indicates that the presented method can not only be used to create F correlated color centers but also that a parasitic effect of neutral vacancy generation is induced. In the following analysis, this allows us to differentiate between these two defects using spectrally resolved PL measurements. Figures 3(b)–3(g) show the corresponding integrated PL intensities obtained for different fs laser pulse properties of the F related centers 3(b)–3(d) and GR1 3(e)–3(g) centers, respectively. The results for the highest (252 kHz) as well as for the lowest (10 kHz) repetition rates suggest an approximately linear increase with increasing pulse energies of both PL intensities in the investigated energy range. As the pulse numbers increase, the PL intensities of both defects also increase. In contrast, for the medium repetition rate (100 kHz), a slightly different behavior can be found. Here, the PL intensities tend to decrease for the highest pulse energies (>60nJ) regardless of the number of pulses. The origin of this drop is unknown. Nevertheless, the PL intensity increases with increasing number of pulses if all other parameters are kept constant. This indicates that the color center formation process is still not saturating in the investigated range of pulse numbers. A trend was also found for laser writing of intrinsic NV centers 15 μm below the diamond surface.[19]

Figures 4(b)–4(i) show the results for the chlorine implanted area. For experimental reasons, measurements could only be performed on the spots made with 252 and 100 kHz. The spectra in this area show mainly a GR1 signature. No PL associated with an additional color center can be found [Figs. 4(d)–4(i)]. The GR1 PL intensity shows an approximately linear increase with increasing pulse energy for all pulse numbers. Similarly to the F related results, the GR1 PL intensity increases with increasing number of pulses if all other parameters remain constant. The absence of PL from additional color centers in this area clearly indicates fluorine related color centers as the second contribution to the PL spectra discussed in the case of F pre-implantation.

It should also be mentioned that in a control experiment on a pristine surface area of the same diamond sample, no change in PL below the damage threshold was found—neither GR1 centers nor other color centers. Similarly, no GR1 PL could be found in the implanted areas without fs laser treatment.

In the following, the absorption behavior of the laser pulses and the associated formation of color centers will be discussed. The findings allow mainly two interpretations. The pre-implantation modifies the diamond lattice in such a way that the absorption dynamics of the fs laser pulses are affected compared to pristine diamond. This enables the creation of vacancies and the rearrangement of these and the pre-implanted ions in the crystal lattice. Alternatively, it could be that the fs-laser pulses do not create any vacancies at all on the surface, or that they are annihilated immediately. Instead, it could be that the

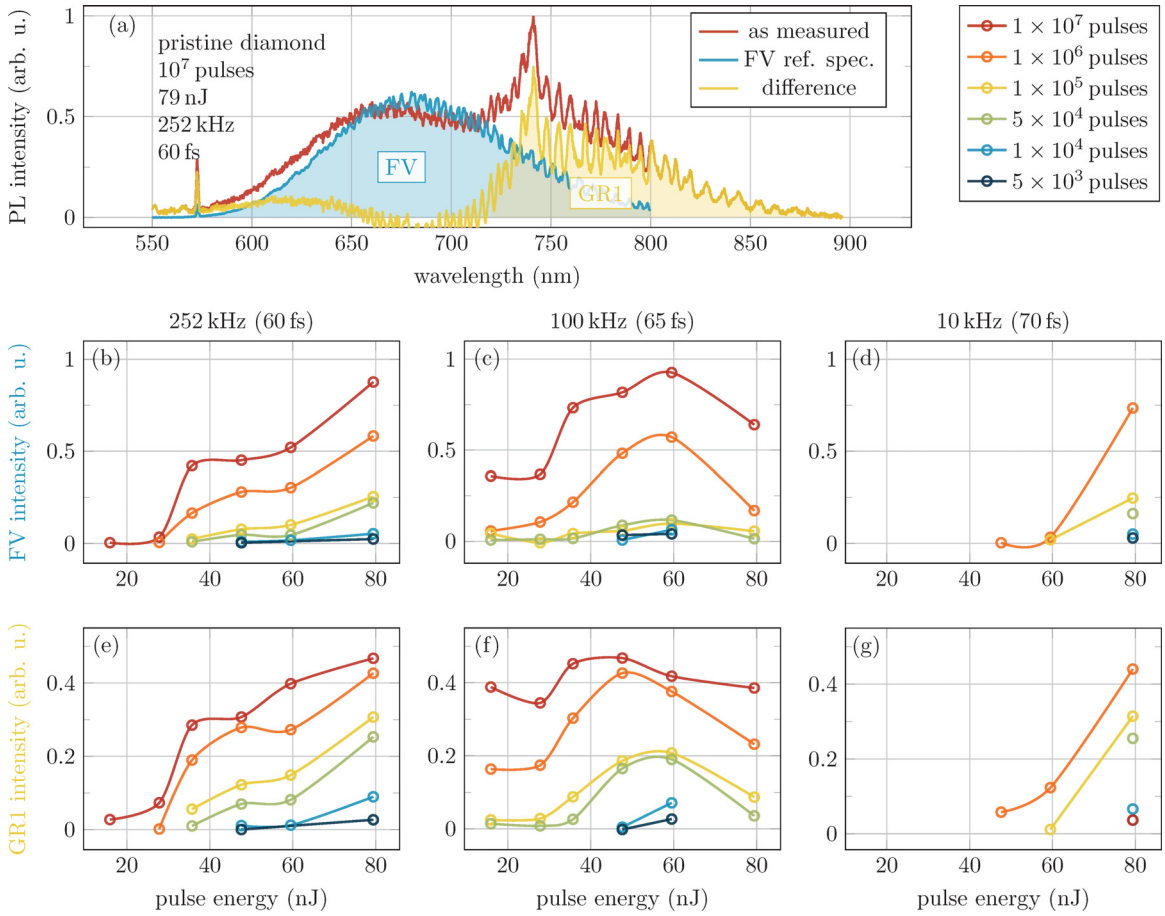

FIG. 3. The results for the fluorine and vacancy related color centers (FV) are shown. (a) An exemplary and background corrected PL spectrum after fs laser treatment on the fluorine pre-implanted area for the parameters given in the inset. The PL spectrum is depicted in red and can be decomposed using an FV reference spectrum obtained by thermal annealing on a separate sample (blue). After subtraction (yellow), the remaining signal shows the spectral signature of GR1 centers. (b)–(g) The integral PL intensities for varying fs laser properties are plotted according to the pale colored areas under the curves in (a). Note that the ripples in the PL spectrum at higher wavelengths are caused by internal reflection inside the spectrometer.

vacancies already created by the ion implantation are recharged to the neutral charge state via the illumination and, thus, become visible in the PL. This is already known for UV illumination.[38] Also here, a kind of diffusion for the vacancies can be assumed, since the presented data show clearly the creation of the FV center in the corresponding region. In both scenarios, this would suggest that GR1 centers are also formed only at the depth of the pre-implantation. Unfortunately, this cannot be verified with the limited depth resolution of a confocal microscope. In any case, the laser pulses appear to lead to the generation of color centers consisting of pre-implanted ions, as demonstrated with fluorine.

Since diamond has a bandgap of 5.4 eV, no linear absorption of visible light can take place. In the bulk, the vacancy generation is, therefore, attributed to non-linear absorption effects, namely, multi-photon ionization and avalanche ionization.[16,17] We could not find such highly nonlinear behavior in our studies. Instead, we found an approximately linear PL increase with increasing pulse energy. One reason for this could be the illumination at the pre-damaged surface. As discussed above, this may result in different optical absorption behavior than in the undamaged bulk, as found in the aforementioned literature. More specifically, this may indicate absorbing interband states arising from the pre-implantation. In addition, the absorption could be strongly dependent on surface properties, like potentially adsorbed molecules or dirt particles. This was minimized by the prior acid cleaning but cannot be ruled out. Finally, we attribute our findings of a linear pulse energy dependency to a more tunneling ionization like effect with subsequent avalanche ionization. The latter scales linear with the laser power.[15] The former also shows a nonlinear behavior. After exceeding an energetic threshold, however, only one first electron has to be generated, so that an avalanche effect can occur. In addition to the adsorbed surface molecules mentioned above, the diamond air interface enables an initial generation of free electrons by ionization of air molecules.[39] In addition, it should be noted that the experimental details, such as the size of the focal spot and the challenge of focusing precisely on the crystal surface, and their interplay can affect the local power input and, thus, the efficiency of color center formation.

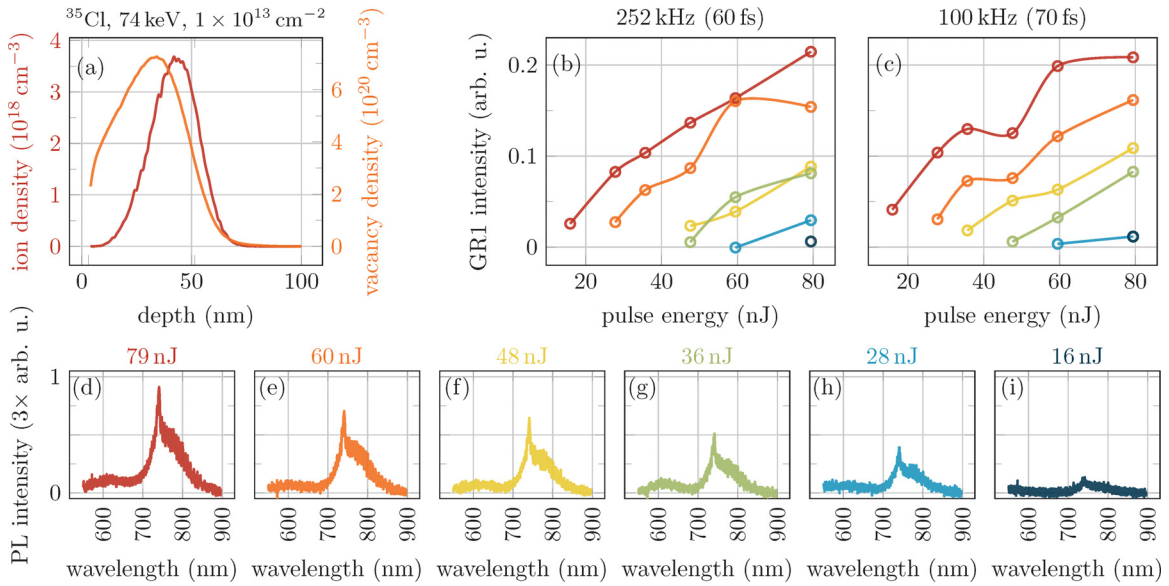

FIG. 4. The results for the chlorine pre-implanted area are shown. (a) The depth dependent ion intensity for chlorine (74keV, 1×10^{13}cm^{-2}). In (b) and (c), the pulse energy dependent PL signal of GR1 centers for different pulse numbers is depicted. The same color coding as in Fig. 3 is used. (d)–(i) The spectral resolved PL of the spots made by 10^7 pulses at 252kHz for different pulse energies. Note that the spectra are scales by a factor of three compared to the normalization used in Fig. 2(i).

The influence of the surface is not limited to the absorption process. In detail, the underlying physics for heat dissipation and for vacancy diffusion at the surface can be assumed to be different from that in the bulk. For example, the spread of the laser induced heat at the surface is different purely by geometry. Since the thermal conductivity in diamond is about 10^5 times higher than in air, effectively only one half-space is available to disperse the heat.[40] For that reason, we claim that fs laser pulses focused on the surface need to have a smaller energy density to induce a vacancy diffusion and a color center formation. Moreover, it is known that the surface acts as a trapping layer for the vacancies and, therefore, reduces the creation yield of shallow and vacancy related defects.[41] Here, the additional creation of shallow vacancies by fs laser pulses opens the way for additional vacancy production with increasing color center creation yield.

The fs timescale of the pulses and the μs timescale of the repetition period lead to a duty cycle of 1.5×10^{-8} (6.5×10^{-9} and 7×10^{-10}). Here, the characteristic cooling time within the focal volume is crucial. For an accumulated heating effect, this should be about the same magnitude as the laser pulse repetition time. The low duty cycle in the presented experiments and the exceptionally high thermal conductivity of diamond, as well as the fact that we always found GR1 centers in the pre-implanted and fs laser treated areas, suggest that a higher repetition rate or longer pulses at lower pulse energies might provide more efficient annealing; in other words, a higher duty cycle with adapted pulse energies might be beneficial.[42]

In conclusion, we combined ion implantation techniques and fs laser treatment for lateral resolved color center formation near the surface of a wideband gap material (depth <100nm). The observations presented above clearly show that fs laser pulses can be used to generate vacancy related color centers in shallow pre-implanted diamond. This technique promises to be applicable to all kinds of color centers and wideband gap semiconductors. However, further optimization of the laser parameters is required. Here, the repetition rate and the duty cycle seem to be crucial. We found a linear dependence of the color center signal on the laser pulse power. This suggests absorbing states in the bandgap generated by the pre-implantation. However, this needs to be verified by further studies. Future studies should also compare laser treatment with conventional annealing, how to combine both and how fs laser pulses can deliver additional vacancies for shallow implanted color centers.

This work was supported by the Director, Office of Science, Office of Basic Energy Sciences, Materials Sciences and Engineering Division, of the U.S. Department of Energy under Contract No. DE-AC02-05-CH11231 within the Nonequilibrium Magnetic Materials Program (MSMAG) (theoretical analysis). K.J., W.L., and T.S, were supported by the Office of Science, Office of Fusion Energy Sciences, of the U.S. Department of Energy, under Contract No. DE-AC02-05CH11231. We also acknowledge support by the National Science Foundation Center for Energy Efficient Electronics Science and the Berkeley Emerging Technology Research (BETR) Center (instrumentation and data acquisition). We acknowledge support from the Leipzig University within the program of Open Access Publishing.

AUTHOR DECLARATIONS

Conflict of Interest

The authors have no conflicts to disclose.

Author Contributions

J.E., M.K., R.W., and T.L. were responsible for the ion implantation. K.J., D.P., and R.W. perform the fs laser treatment. T.S. and J.B. supervised the fs laser experiments. W.L. gave first insight into the confocal

PL measurements. R.W. supervised all experimental steps, performed the analysis, and wrote the manuscript.

Johannes Engel: Investigation (equal); Writing – review & editing (equal). **Kaushalya Jhuria:** Investigation (equal); Writing – review & editing (equal). **Debanjan Polley:** Investigation (equal); Writing – review & editing (equal). **Tobias Lühmann:** Investigation (equal); Writing – review & editing (equal). **Manuel Kuhrke:** Investigation (equal). **Wei Liu:** Investigation (equal). **Jeffrey Bokor:** Supervision (equal). **Thomas Schenkel:** Supervision (equal). **Ralf Wunderlich:** Conceptualization (equal); Formal analysis (equal); Investigation (equal); Methodology (equal); Project administration (equal); Software (equal); Supervision (equal); Visualization (equal); Writing – original draft (equal).

DATA AVAILABILITY

The data that support the findings of this study are available from the corresponding author upon reasonable request.

REFERENCES

[1]M. W. Doherty, N. B. Manson, P. Delaney, F. Jelezko, J. Wrachtrup, and L. C. Hollenberg, "The nitrogen-vacancy colour centre in diamond," Phys. Rep. **528**(1), 1 (2013).
[2]S. Pezzagna and J. Meijer, Appl. Phys. Rev. **8**, 011308 (2021).
[3]S. Castelletto and A. Boretti, J. Phys.: Photonics **2**, 022001 (2020).
[4]T. Lühmann, N. Raatz, R. John, M. Lesik, J. Rödiger, M. Portail, D. Wildanger, F. Kleißer, K. Nordlund, A. Zaitsev, J.-F. Roch, A. Tallaire, J. Meijer, and S. Pezzagna, J. Phys. D: Appl. Phys. **51**, 483002 (2018).
[5]M. Rühl, C. Ott, S. Götzinger, M. Krieger, and H. B. Weber, Appl. Phys. Lett. **113**, 122102 (2018).
[6]J. O. Orwa, C. Santori, K. M. C. Fu, B. Gibson, D. Simpson, I. Aharonovich, A. Stacey, A. Cimmino, P. Balog, M. Markham, D. Twitchen, A. D. Greentree, R. G. Beausoleil, and S. Prawer, J. Appl. Phys. **109**, 083530 (2011).
[7]S. Pezzagna, D. Rogalla, D. Wildanger, J. Meijer, and A. Zaitsev, New J. Phys. **13**, 035024 (2011).
[8]J. M. Smith, S. A. Meynell, A. C. B. Jayich, and J. Meijer, Nanophotonics **8**, 1889 (2019).
[9]J. Martin, R. Wannemacher, J. Teichert, L. Bischoff, and B. Köhler, Appl. Phys. Lett. **75**, 3096 (1999).
[10]D. M. Toyli, C. D. Weis, G. D. Fuchs, T. Schenkel, and D. D. Awschalom, Nano Lett. **10**, 3168 (2010).
[11]K. Groot-Berning, T. Kornher, G. Jacob, F. Stopp, S. T. Dawkins, R. Kolesov, J. Wrachtrup, K. Singer, and F. Schmidt-Kaler, Phys. Rev. Lett. **123**, 106802 (2019).
[12]P. Räcke, R. Wunderlich, J. W. Gerlach, J. Meijer, and D. Spemann, New J. Phys. **22**, 083028 (2020).
[13]L. C. Courrol, R. E. Samad, L. Gomes, I. M. Ranieri, S. L. Baldochi, A. Z. de Freitas, and N. D. V. Junior, Opt. Express **12**, 288 (2004).
[14]A. Hertwig, S. Martin, J. Krüger, and W. Kautek, Appl. Phys. A **79**, 1075 (2004).
[15]S. Castelletto, J. Maksimovic, T. Katkus, T. Ohshima, B. C. Johnson, and S. Juodkazis, Nanomaterials **11**, 72 (2020).
[16]X.-J. Wang, H.-H. Fang, F.-W. Sun, and H.-B. Sun, Laser Photonics Rev. **16**, 2100029 (2022).
[17]Y.-C. Chen, P. S. Salter, S. Knauer, L. Weng, A. C. Frangeskou, C. J. Stephen, S. N. Ishmael, P. R. Dolan, S. Johnson, B. L. Green, G. W. Morley, M. E. Newton, J. G. Rarity, M. J. Booth, and J. M. Smith, Nat. Photonics **11**, 77 (2017).
[18]Y.-C. Chen, B. Griffiths, L. Weng, S. S. Nicley, S. N. Ishmael, Y. Lekhai, S. Johnson, C. J. Stephen, B. L. Green, G. W. Morley, M. E. Newton, M. J. Booth, P. S. Salter, and J. M. Smith, Optica **6**, 662 (2019).
[19]T. Kurita, Y. Shimotsuma, M. Fujiwara, M. Fujie, N. Mizuochi, M. Shimizu, and K. Miura, Appl. Phys. Lett. **118**, 214001 (2021).
[20]S. Castelletto, A. F. M. Almutairi, K. Kumagai, T. Katkus, Y. Hayasaki, B. C. Johnson, and S. Juodkazis, Opt. Lett. **43**, 6077 (2018).
[21]Y.-C. Chen, P. S. Salter, M. Niethammer, M. Widmann, F. Kaiser, R. Nagy, N. Morioka, C. Babin, J. Erlekampf, P. Berwian, M. J. Booth, and J. Wrachtrup, Nano Lett. **19**, 2377 (2019).
[22]A. F. M. Almutairi, J. G. Partridge, C. Xu, I. S. Cole, and A. S. Holland, Appl. Phys. Lett. **120**, 014003 (2022).
[23]J. Liu, Z. Xu, Y. Song, H. Wang, B. Dong, S. Li, J. Ren, Q. Li, M. Rommel, X. Gu, B. Liu, M. Hu, and F. Fang, Nanotechnol. Precis. Eng. **3**, 218 (2020).
[24]J. Lang, S. Häußler, J. Fuhrmann, R. Waltrich, S. Laddha, J. Scharpf, A. Kubanek, B. Naydenov, and F. Jelezko, Appl. Phys. Lett. **116**, 064001 (2020).
[25]A. Healey, L. Hall, G. White, T. Teraji, M.-A. Sani, F. Separovic, J.-P. Tetienne, and L. Hollenberg, Phys. Rev. Appl. **15**, 054052 (2021).
[26]Y. Romach, C. Müller, T. Unden, L. J. Rogers, T. Isoda, K. M. Itoh, M. Markham, A. Stacey, J. Meijer, S. Pezzagna, B. Naydenov, L. P. McGuinness, N. Bar-Gill, and F. Jelezko, Phys. Rev. Lett. **114**, 017601 (2015).
[27]M. Loretz, S. Pezzagna, J. Meijer, and C. L. Degen, Appl. Phys. Lett. **104**, 033102 (2014).
[28]N. Aslam, M. Pfender, P. Neumann, R. Reuter, A. Zappe, F. F. de Oliveira, A. Denisenko, H. Sumiya, S. Onoda, J. Isoya, and J. Wrachtrup, Science **357**, 67 (2017).
[29]S. Kawai, H. Yamano, T. Sonoda, K. Kato, J. J. Buendia, T. Kageura, R. Fukuda, T. Okada, T. Tanii, T. Higuchi, M. Haruyama, K. Yamada, S. Onoda, T. Ohshima, W. Kada, O. Hanaizumi, A. Stacey, T. Teraji, S. Kono, J. Isoya, and H. Kawarada, J. Phys. Chem. C **123**, 3594 (2019).
[30]F. Jelezko and J. Wrachtrup, Phys. Status Solidi (a) **203**, 3207 (2006).
[31]I. Harris, C. J. Ciccarino, J. Flick, D. R. Englund, and P. Narang, Phys. Rev. B **102**, 195206 (2020).
[32]K. Liu, S. Zhang, V. Ralchenko, P. Qiao, J. Zhao, G. Shu, L. Yang, J. Han, B. Dai, and J. Zhu, Adv. Mater. **33**, 2000891 (2021).
[33]S. Ditalia Tchernij, T. Lühmann, E. Corte, F. Sardi, F. Picollo, P. Traina, M. Brajkovic, A. Crnjac, S. Pezzagna, Z. Pastuovic, I. P. Degiovanni, E. Moreva, P. Aprà, P. Olivero, Z. Siketic, J. Meijer, M. Genovese, and J. Forneris, Sci. Rep. **10**, 21537 (2020).
[34]J. P. Goss, P. R. Briddon, M. J. Rayson, S. J. Sque, and R. Jones, Phys. Rev. B **72**, 035214 (2005).
[35]J. F. Ziegler, M. Ziegler, and J. Biersack, Nucl. Instrum. Methods **268**, 1818 (2010).
[36]J. Lowther, J. Phys. Chem. Solids **45**, 127 (1984).
[37]S. Subedi, V. Fedorov, S. Mirov, and M. Markham, Opt. Mater. Express **11**, 757 (2021).
[38]H. B. Dyer and L. d Preez, J. Chem. Phys. **42**, 1898 (1965).
[39]Y. Liu, G. Chen, M. Song, X. Ci, B. Wu, E. Wu, and H. Zeng, Opt. Express **21**, 12843 (2013).
[40]D. Twitchen, C. Pickles, S. Coe, R. Sussmann, and C. Hall, Diamond Related Mater. **10**, 731 (2001).
[41]P. Räcke, L. Pietzonka, J. Meijer, D. Spemann, and R. Wunderlich, Appl. Phys. Lett. **118**, 204003 (2021).
[42]Y. Xu, R. Wang, S. Ma, L. Zhou, Y. R. Shen, and C. Tian, J. Appl. Phys. **123**, 025301 (2018).